An Example-Based Face Hallucination Method for Single-Frame, Low-Resolution Facial Images

Jeong-Seon Park, *Member, IEEE*, and Seong-Whan Lee, *Senior Member, IEEE*

***Abstract*—This paper proposes a face hallucination method for the reconstruction of high-resolution facial images from single-frame, low-resolution facial images. The proposed method has been derived from example-based hallucination methods and morphable face models. First, we propose a recursive error back-projection method to compensate for residual errors, and a region-based reconstruction method to preserve characteristics of local facial regions. Then, we define an extended morphable face model, in which an extended face is composed of the interpolated high-resolution face from a given low-resolution face, and its original high-resolution equivalent. Then, the extended face is separated into an extended shape and an extended texture. We performed various hallucination experiments using the MPI, XM2VTS, and KF databases, compared the reconstruction errors, structural similarity index, and recognition rates, and showed the effects of face detection errors and shape estimation errors. The encouraging results demonstrate that the proposed methods can improve the performance of face recognition systems. Especially the proposed method can enhance the resolution of single-frame, low-resolution facial images.**

***Index Terms*—Error back-projection, example-based reconstruction, extended morphable face model, face hallucination, face recognition, region-based reconstruction.**

I. Introduction

HANDLING low-resolution images is one of the most difficult problems commonly encountered in various kinds of image processing applications, such as the generation of 3-D models, analysis of scientific/medical/astronomical/weather images, archiving, retrieval, and transmission of these images, video surveillance, and monitoring [1]. Numerous methods involving the synthesis or reconstruction of high-resolution images from either a sequence of low-resolution images or a single-frame, low-resolution image have been reported [2].

Interpolations are typical approaches for generating a magnified image, by reproducing existing pixels and smoothing the new image. However, the performance of such direct interpolations is usually poor, since no new information is included into the process [3]. In contrast to interpolations, super-resolutions increase the resolution of a video frame using the relation of neighboring frames [4]–[6]. Super-resolutions are roughly separated into two classes according to the type of applied low-resolution images: general super-resolution, which extracts a single high-resolution image from a sequence of general low-resolution images [7], and domain specific super-resolution, which extracts high-resolution image details from a restricted class of low-resolution images, such as in the face domain.

Super-resolution approaches [3], [7]–[17] generally depend on prior knowledge of the image class to be reconstructed. These techniques involve designing a co-occurrence model using a training set of high-resolution images and their low-resolution counterparts. In example-based learning methods, the aim is to predict high-resolution data from the observed low-resolution data. Hardie *et al.* [7] and Stephenson and Chen [8] used Markov random field (MRF) priors, which are generally applied to generic images.

However, for face hallucination, domain knowledge about facial images was used to generate high-resolution facial images. Baker and Kanade [1] adopted an image pyramid to predict a prior under a Bayesian formulation. This method derives high-frequency components from a parent structure with training samples. Gunturk *et al.* [9] applied principal component analysis (PCA) to determine the prior model. Wang and Tang [3] developed a face hallucination algorithm using an Eigen transformation. However, this method only utilizes global information without paying attention to local details. Liu *et al.* [10] proposed a two-step approach, which integrates a parametric global model with Gaussian assumptions and linear inference, and a nonparametric local model based on MRF. Motivated by Liu *et al.*, Li and Lin [11] also proposed a two-step approach for hallucinating faces by reconstructing a global image with a Maximum A Posterior (MAP) criterion and re-estimating a residual image with the MAP criterion. They also attempted to overcome pose variation by applying pose estimation using support vector machine (SVM), where 21 landmarks are defined for each facial image [12]. A Tensor-Patch-based method, in which 682 overlapped patches are used for hallucination and PCA compensates for the residual error, was also proposed in [13]. They also applied a similar method to synthesize facial images from sketch images [14].

We attempted to reconstruct high-resolution facial images from single-frame, low-resolution facial images using the recursive error back-projection method [15]. This method recursively updates a reconstructed high-resolution image by estimating a high-resolution image, simulating a low-resolution image from

Manuscript received May 4, 2007; revised May 1, 2008. Current version published September 10, 2008. This work was supported by the Ministry of Knowledge Economy, Korea, under the ITRC (Information Technology Research Center) support program supervised by the IITA (Institute of Information Technology Advancement) (IITA-2008-C1090-0801-0001) and the Intelligent Robotics Development Program, one of the 21st Century Frontier R&D Programs funded by the Ministry of Commerce, Industry and Energy of Korea. The associate editor coordinating the review of this manuscript and approving it for publication was Dr. Dimitri Van De Ville.

J.-S. Park is with the Department of Multimedia, Chonnam National University, Dundeok-dong, Yosu, Jeollanam-do 550-749, Korea (e-mail: jpark@chonnam.ac.kr).

S.-W. Lee is with the Department of Computer Science and Engineering, Korea University, Anam-dong, Seongbuk-ku, Seoul 136-713, Korea (e-mail: swlee@image.korea.ac.kr).

Color versions of one or more of the figures in this paper are available online at http://ieeexplore.ieee.org.

Digital Object Identifier 10.1109/TIP.2008.2001394

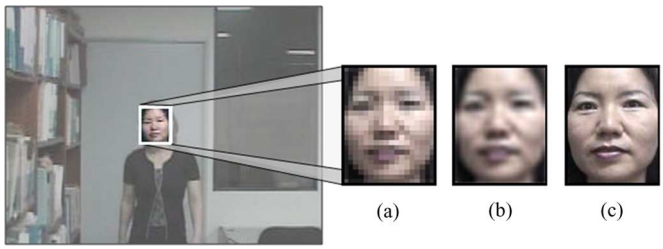

Fig. 1. Example of a low-resolution facial image from a single-frame image: (a) cropped low-resolution facial image, (b) resolution-enhanced facial image by bicubic interpolation, and (c) desired high-resolution facial image.

an estimated high-resolution image, and compensating for high-resolution errors in order to reduce residual errors.

In this study, we propose a new region-based reconstruction method for preserving the characteristics of the local facial regions. The proposed face hallucination method is applied to an extended morphable face model, whereas most existing approaches are applied to general face models, for which a face is only represented by pixel values in a normalized facial image. In the proposed extended morphable face model, an extended face is defined by the combination of the interpolated high-resolution face from a given low-resolution face, and its original high-resolution face. Then, the extended face is separated into an extended shape and an extended texture.

Section II introduces the basic concept of the classic, example-based reconstruction method and the existing morphable face models. In Section III, we propose an example-based face hallucination method and provide a mathematical procedure for solving example-based reconstruction problems. We implement a recursive error back-projection method to compensate for residual errors, and a region-based reconstruction method to preserve characteristics of local regions. We define an extended morphable face model for face hallucination problems. Section IV presents and analyzes the experimental results with low-resolution facial images. Finally, conclusion and future research are discussed in Section V.

II. Related Work

Before describing the proposed example-based face hallucination method, we introduce the concept of example-based reconstruction methods that use domain knowledge derived from numerous example faces. We also describe existing morphable face models [18], [19], which were reported as more powerful models for representing a facial image than other general face models [20].

Many video applications, such as surveillance or monitoring systems must extract and enhance small faces from a sequence of low-resolution frames [21], [22]. Face detection is one of important research issue, as extensively surveyed by Yang *et al.* [23] and Kakumanua *et al.* [24]. Because algorithmic face detection is beyond the scope of this work, we assume that facial images were previously extracted and cropped, as shown in Fig. 1.

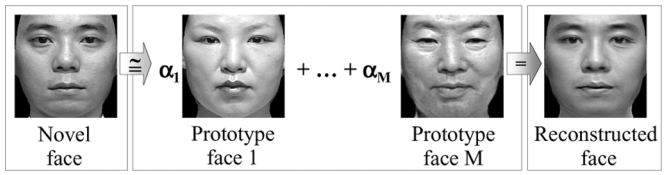

Fig. 2. Concept of example-based face reconstruction: Any novel face can be approximated by a linear combination of prototype faces.

A. Example-Based Face Reconstruction Method

Assume that a sufficiently large number of facial images are available for offline training, and that we can build prototype faces that can represent any novel facial image by a linear combination of these prototypes [18]–[20], as shown in Fig. 2.

In order to describe the mathematical procedure for the example-based reconstruction method above, the following notations are defined. First, a novel (or input) facial image ($\mathbf{I}$) is represented by a column vector of all pixel values, as follows:

$$\mathbf{I} = (i_1, i_2, \ldots, i_n, \ldots, i_N)^{\mathrm{T}} \in \Re^N \tag{1}$$

where i_n is the intensity or color of the nth pixel, x_n, among N pixels in the facial image and $\mathbf{I}(x_n)$ represents the pixel value of x_n, i.e., $\mathbf{I}(x_n) = i_n$.

We denote the reconstructed face as $\mathbf{R}$, which is obtained by a linear combination of M prototype faces for the input facial image $\mathbf{I}$. The above example-based reconstruction method is represented by the following linear equation:

$$\mathbf{I} \cong \alpha_1\mathbf{P}_1 + \alpha_2\mathbf{P}_2 + \cdots + \alpha_M\mathbf{P}_M = \sum_{m=1}^{M} \alpha_m\mathbf{P}_m = \mathbf{R} \tag{2}$$

where $\mathbf{P}_m$ and α_m are mth prototype face and its coefficient value, respectively.

If we define the parameter set as a vector $\vec{\boldsymbol{\alpha}} = (\alpha_1, \alpha_2, \ldots, \alpha_M)^T$ and prototype faces as a matrix $\mathbf{P} = (\mathbf{P}_1, \mathbf{P}_2, \ldots, \mathbf{P}_M)$, (2) is reformulated as the following simple inner product:

$$\mathbf{R} = \mathbf{P} \cdot \vec{\boldsymbol{\alpha}}. \tag{3}$$

We applied PCA to example facial images in order to transform the image coordinate system to the orthogonal coordinate system. In the orthogonal coordinate system, any facial image is decomposed into a linear combination of eigenvectors $(\mathbf{e}_1, \mathbf{e}_2, \ldots, \mathbf{e}_M)$ of the covariance matrix. The covariance matrix is computed from differences between the set of example facial images and the mean image ($\bar{\mathbf{I}}$) of these training facial images. Then, a novel facial image is represented by the following equation:

$$\Delta\mathbf{I} = \mathbf{I} - \bar{\mathbf{I}} = \sum_{m=1}^{M} \alpha_m\mathbf{e}_m \Rightarrow \mathbf{I} = \bar{\mathbf{I}} + \sum_{m=1}^{M} \alpha_m\mathbf{e}_m \tag{4}$$

where $\Delta\mathbf{I}$ is the difference vector between the mean and trainig images.

From (4), it can be shown that the eigenvectors or eigenfaces $(\mathbf{e}_1, \mathbf{e}_2, \ldots, \mathbf{e}_M)$ are considered as facial prototypes in the example-based reconstruction method, by a simple modification of difference vectors. In the following sections, we assume that $\mathbf{P} = (\mathbf{P}_1, \mathbf{P}_2, \ldots, \mathbf{P}_M)$ are M eigenfaces $(\mathbf{e}_1, \mathbf{e}_2, \ldots, \mathbf{e}_M)$, in order to simplify the mathematical procedure for example-based reconstruction method.

In order to determine the optimal parameter set, we select a parameter set $\vec{\boldsymbol{\alpha}}$, such that the reconstruction error is minimized. For this, we define an error function $\mathbf{E}(\vec{\boldsymbol{\alpha}})$ as the sum of the square of errors, which represents the difference between the input facial image and its reconstructed equivalent, as follows:

$$\begin{aligned}\mathbf{E}(\vec{\boldsymbol{\alpha}}) &= \sum_{n=1}^{N} (\mathbf{I}(x_n) - \mathbf{R}(x_n))^2 = \|\mathbf{I} - \mathbf{R}\|^2 \\ &= \|\mathbf{I} - \vec{\boldsymbol{\alpha}} \cdot \mathbf{P}\|^2 \end{aligned} \tag{5}$$

where $\mathbf{I}$ and $\mathbf{R}$ are the column vectors of N pixels, $x_1, x_2, \ldots, x_N$, of an input facial image and a reconstructed image, respectively.

Then, the problem of reconstruction is equivalent to the determination of $\vec{\hat{\boldsymbol{\alpha}}}$, which minimizes the above error function as follows:

$$\vec{\boldsymbol{\alpha}}^* = \arg\min_{\vec{\boldsymbol{\alpha}}} \mathbf{E}(\vec{\boldsymbol{\alpha}}). \tag{6}$$

B. Morphable Face Model

Morphable face models, introduced by Vetter and Troje [18] and extended by 3-D morphable face model, were very successful at encoding, representing, or recognizing human facial images [19], [20]. In this model, a facial image is separated into a shape vector and a texture vector. Assuming that the pixel-wise correspondence between facial images was previously established [18], the 2-D shape of a face is coded as displacement fields in a reference face.

In many example-based applications, the accuracy of normalization affects performance. General face models only use pixel values, which are only aligned according to a few features such as the eyes, nose, and mouth in the normalized facial image, whereas the morphable face model is considered as the most accurate normalization method, in the sense that the positions of all pixels are adjusted according to the reference face, then, pixel values (texture) of the normalized face and displacement values (shape) are coded. Thus, the morphable face model yields the same volume of shape and texture information in the reference face. In addition, this model could potentially represent any novel face and synthesize a new face, by using the example shape and texture vectors.

The shape of a facial image is represented by the following vector:

$$\mathbf{S} = (d_1^x, d_1^y, \ldots, d_n^x, d_n^y, \ldots, d_N^x, d_N^y)^{\mathrm{T}} \in \Re^{2N} \tag{7}$$

where N is the number of pixels in a facial image, and (d_n^x, d_n^y) is the x, y displacement of a pixel that corresponds to pixel x_n in the reference face, denoted by $\mathrm{S}(x_n)$.

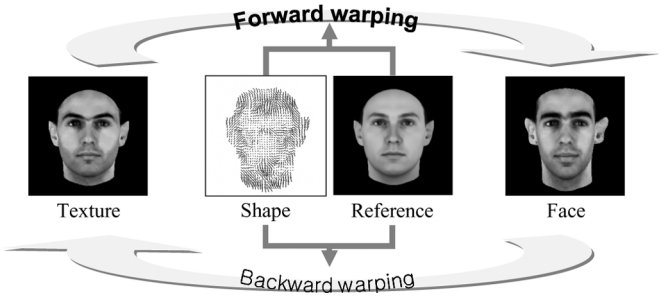

Fig. 3. Examples of forward and backward warping.

The texture is coded as the intensity map of the image, resulting from mapping the face image to the reference face. Thus, the normalized (shape free) texture is represented as the following vector:

$$\mathbf{T} = (i_1, \ldots, i_n, \ldots, i_N)^{\mathrm{T}} \in \Re^N \tag{8}$$

where i_n is the intensity or color of the nth pixel that corresponds to pixel x_n among N pixels in the reference face, denoted by $\mathrm{T}(x_n)$.

Then, by applying the basic concept of the example-based reconstruction method to both the shape and texture vectors, both vectors are expressed as the following linear combinations of prototypes:

$$\mathbf{S} \cong \vec{\boldsymbol{\beta}} \cdot \mathbf{S}^{\mathbf{P}}, \quad \mathbf{T} \cong \vec{\boldsymbol{\gamma}} \cdot \mathbf{T}^{\mathbf{P}} \tag{9}$$

where $\mathbf{S}$ and $\mathbf{T}$ are the shape and texture vectors of the facial image, $\mathbf{S}^{\mathbf{P}}$ and $\mathbf{T}^{\mathbf{P}}$ are the prototype shape (eigen-shape) vectors and prototype texture (eigen-texture) vectors constructed from examples of the shape and texture vectors, and $\vec{\boldsymbol{\beta}}$ and $\vec{\boldsymbol{\gamma}}$ are coefficient vectors for linear combinations of prototype shape and texture vectors, respectively.

In order to understand and apply the morphable face model, we must understand the two kinds of warping processes: forward and backward warping (refer to Fig. 3). Forward warping (texture warping) warps the texture expressed in the reference face to each face image using its shape information. This generates a face image. Backward warping warps a face image to the reference face using its shape information. This generates the texture information expressed in the reference face. The mathematical definition and further details about the forward and backward warping are found in Vetter and Troje's research [18].

III. Proposed Face Hallucination Method

In this section, we describe a mathematical solution for example-based face hallucination, a recursive error back-projection method which compensates for residual errors, and a region-based reconstruction method for preserving characteristics of local facial regions. Then, we define an extended morphable face model, for which an extended face is composed of the interpolated high-resolution face from a given low-resolution face, and its original high-resolution equivalent, then, separated into an extended shape and an extended texture.

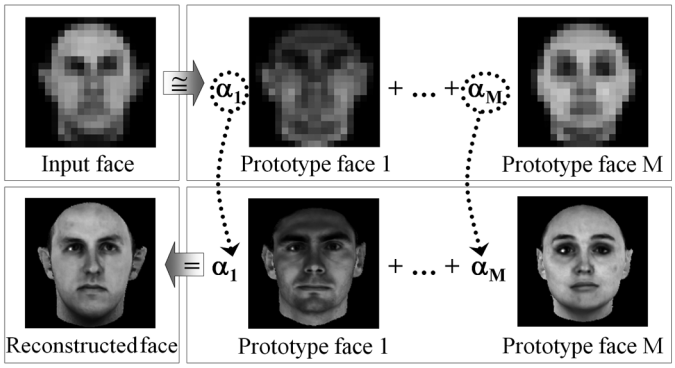

Fig. 4. Basic concept of the example-based face hallucination method: A high-resolution face is reconstructed as a linear combination of high-resolution prototype faces by finding the optimal solution from the given low-resolution face.

A. Example-Based Face Hallucination Method

In order to apply the example-based, face reconstruction method to single-frame face hallucination, we assume that pairs of low-resolution facial images and their corresponding high-resolution facial equivalents are collected.

From the definition of the example-based reconstruction method, we obtain an approximation to the deformation required for the given low-resolution face, using coefficients of low-resolution prototype faces. Then, a high-resolution face is obtained by applying the estimated coefficients to the corresponding high-resolution prototype faces, as shown in Fig. 4.

Consequently, our aim is to find an optimal parameter set $(\vec{\alpha})$ that best represents the given low-resolution facial image as a linear combination of low-resolution prototype faces. Equivalently, we require an approximation to the deformation for the input face using coefficients of the low-resolution prototype faces.

In order to obtain the optimal parameter set $\vec{\alpha}$, we define an extended face $\mathbf{I}^+$ by concatenating a low-resolution face $\mathbf{I_L}$ and its high-resolution equivalent $(\mathbf{I_H})$, as follows:

$$\mathbf{I}^+ = (i_1, i_2, \ldots, i_L, i_{L+1}, i_{L+2}, \ldots, i_{L+H})^{\mathrm{T}} \tag{10}$$

where L and H are the number of pixels in the low-resolution, $\mathbf{I_L} = (i_1, i_2, \ldots, i_L)^{\mathrm{T}}$ and the high-resolution, $\mathbf{I_H} = (i_1, i_2, \ldots, i_H)^{\mathrm{T}}$ facial images, respectively.

An extended facial image $\mathbf{I}^+$ is represented by a linear combination of extended prototype faces by applying the following example-based reconstruction method:

$$\mathbf{I}^+ \cong \mathbf{P}^+ \cdot \vec{\alpha} = \mathbf{R}^+ \tag{11}$$

where $\mathbf{P}^+$ and $\mathbf{R}^+$ are the extended prototype faces and reconstructed facial image, respectively.

The above equation is similar to (3). However, for face hallucination problem, only L pixels of the low-resolution face are provided, among the $L + H$ pixels of the extended face. The remaining problem is determining the M coefficient values. In order to obtain an optimal parameter set $\vec{\alpha}$, we define a similar error function, $\mathrm{E}_{\mathbf{L}}^+(\vec{\alpha})$ comprising the sum of the square of errors between the given low-resolution pixels and their reconstructed pixels, for the low-resolution component of the extended face, as follows:

$$\begin{aligned}\mathrm{E}_{\mathbf{L}}^+(\vec{\alpha}) &= \sum_{n=1}^{L} \left(\mathbf{I}^+(x_n) - \mathbf{R}_{\mathbf{L}}^+(x_n)\right)^2 \\ &= \sum_{n=1}^{L} \left(\mathbf{I}^+(x_n) - \vec{\alpha} \cdot \mathbf{P}_{\mathbf{L}}^+(x_n)\right)^2 = \|\mathbf{I}_{\mathbf{L}}^+ - \mathbf{P}_{\mathbf{L}}^+ \cdot \vec{\alpha}\|^2\end{aligned} \tag{12}$$

where $\mathbf{I}_{\mathbf{L}}^+$, $\mathbf{P}_{\mathbf{L}}^+$, and $\mathbf{R}_{\mathbf{L}}^+$ are the low-resolution component of the extended face, the extended prototype faces, and the extended reconstructed face, respectively.

Then, the problem of face hallucination is equivalent to determination of $\vec{\alpha}^*$, which minimize the above error function, as follows:

$$\vec{\alpha}^* = \arg\min_{\vec{\alpha}} \mathrm{E}_{\mathbf{L}}^+(\vec{\alpha}). \tag{13}$$

In order to obtain an optimal solution, we assume that an optimal solution satisfies the following constraint, where ε is a suitably small constant value such as PCA reconstruction error

$$\mathrm{E}_{\mathbf{L}}^+(\vec{\alpha}) \leq \varepsilon. \tag{14}$$

If ε is a suitably small reconstruction error, then this term is negligible for finding an optimal solution, and (12) is substituted in the above equation. We solve (14) by the following matrix form:

$$\mathbf{I}_{\mathbf{L}}^+ = \mathbf{P}_{\mathbf{L}}^+ \cdot \vec{\alpha}. \tag{15}$$

According to the characteristics of inner product and transposition of a matrix, the above equation is expanded as follows:

$$(\mathbf{P}_{\mathbf{L}}^+)^{\mathrm{T}} \cdot \mathbf{P}_{\mathbf{L}}^+ \cdot \vec{\alpha} = (\mathbf{P}_{\mathbf{L}}^+)^{\mathrm{T}} \cdot \mathbf{I}_{\mathbf{L}}^+. \tag{16}$$

If the columns of $\mathbf{P}_{\mathbf{L}}^+$ are linearly independent and the determinant of $\mathbf{P}_{\mathbf{L}}^+$ is nonzero, the term $(\mathbf{P}_{\mathbf{L}}^+)^{\mathrm{T}} \cdot \mathbf{P}_{\mathbf{L}}^+$ is nonsingular, and there exist an inverse. Then, the optimal solution is obtained by the following equation:

$$\vec{\alpha}^* = \left((\mathbf{P}_{\mathbf{L}}^+)^{\mathrm{T}} \cdot \mathbf{P}_{\mathbf{L}}^+\right)^{-1} \cdot (\mathbf{P}_{\mathbf{L}}^+)^{\mathrm{T}} \cdot \mathbf{I}_{\mathbf{L}}^+. \tag{17}$$

Then, an extended reconstruction face $\mathbf{R}^+$ is obtained by applying the obtained parameter $\vec{\alpha}^*$ to the extended prototype faces $\mathbf{P}^+$, i.e., $\mathbf{R}^+ = \mathbf{P}^+ \cdot \vec{\alpha}^*$.

Finally, we obtain a high-resolution facial image by considering H pixels in the high-resolution component of the extended reconstruction face, as follows:

$$\mathbf{R_H}(x_j) = \mathbf{R}^+(x_{L+j}), \quad j = 1, 2, \ldots, H \tag{18}$$

where $x_1, \ldots, x_H$ are pixels in the reconstructed high-resolution facial image.

Using these procedures, it is possible to obtain a high-resolution facial image from any new low-resolution facial image. The concept of example-based face

hallucination is summarized by the following equation:

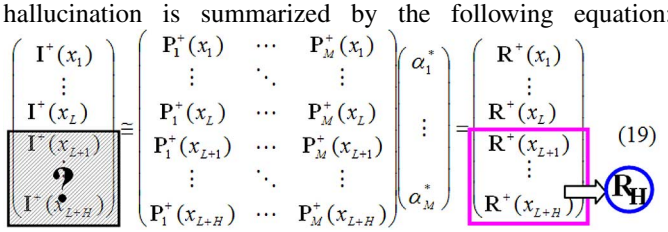

(19)

B. Recursive Error Back-Projection Method

According to the previous example-based reconstruction method, we approximate a given low-resolution facial image with errors, as defined by (12) of the estimated $\vec{\alpha}^*$. Therefore, it seems likely that the reconstructed high-resolution facial image involves the following errors:

$$\begin{aligned} \mathrm{E}_{\mathbf{H}}^{+}(\vec{\alpha}) &= \|\mathbf{I}_{\mathbf{H}}^{+} - \vec{\alpha}\cdot\mathbf{P}_{\mathbf{H}}^{+}\|^2 \\ &= \sum_{n=1}^{H}\left(\mathbf{I}_{\mathbf{H}}^{+}(x_n) - \vec{\alpha}^*\cdot\mathbf{P}_{\mathbf{H}}^{+}(x_n)\right)^2 \end{aligned} \tag{20}$$

where $\mathbf{I}_{\mathbf{H}}^{+}$ (in fact, the real high-resolution facial image is unknown), $\mathbf{P}_{\mathbf{H}}^{+}$, and $\mathbf{R}_{\mathbf{H}}^{+}$ are the high-resolution component of the extended facial image, the extended prototype faces, and the reconstructed facial image, respectively.

In order to compensate for the residual errors above, we applied a recursive error back-projection procedure to the example-based face hallucination method. The proposed recursive error back-projection method is applied to reduce the face hallucination error. This recursively compensates for high-resolution errors, which is estimated by a similar example-based reconstruction method from the estimated low-resolution difference. A flow-chart of the procedure for recursive error back-projection is given in Fig. 5.

Terms used in Fig. 5 are defined as follows.

$\mathbf{I}_{\mathrm{L}}$	*Input low-resolution vector*
t	*Iteration index, t=1, 2, …, T*
$\mathbf{R}_{\mathbf{H}}^{t}$	*Reconstructed high-resolution vector during iteration t*
$\mathbf{R}_{\mathbf{H}}^{\min}$	*Current optimal high-resolution vector with minimum reconstruction error during iterations*
$\mathbf{R}_{\mathbf{L}}^{t}$	*Simulated low-resolution vector by down-sampling the reconstructed high-resolution vector during iteration t*
$\mathbf{E}_{\mathbf{L}}^{t}$	*Reconstruction error by measuring the Euclidean distance between the input low-resolution vector and the simulated low-resolution vector during iteration t*
$\mathbf{E}_{\mathbf{L}}^{\min}$	*Minimum reconstruction error from the initial estimation to the current iteration*
δ_1	*Threshold value to determine whether the current reconstruction is accurate*
δ_2	*Threshold value to determine whether the current iteration is inferior*
δ_3	*Threshold value to determine whether the current iteration is convergent*
$\mathbf{D}_{\mathbf{L}}^{t}$	*Low-resolution difference vector by measuring the pixel-wise difference between an input low-resolution vector and the simulated low-resolution vector during iteration t*
$\mathbf{D}_{\mathbf{H}}^{t}$	*High-resolution difference vector reconstructed from the low-resolution difference vector by example-based reconstruction during iteration t*
w_t	*Weight value for error compensation during iteration t*

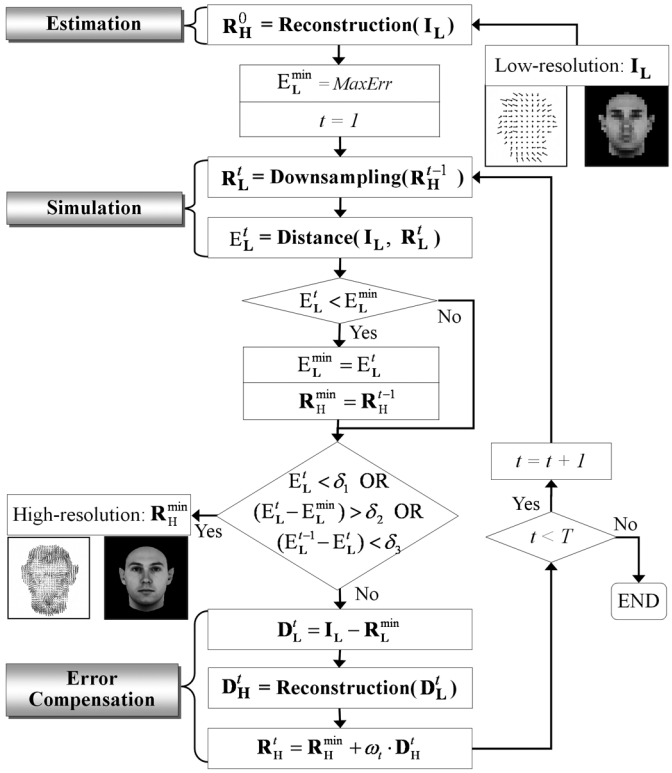

Fig. 5. Proposed recursive error back-projection method: The initially reconstructed high-resolution facial image is recursively compensated for by the estimated high-resolution difference vectors.

In the initial stage, we reconstruct the high-resolution vector $(\mathbf{R}_{\mathbf{H}}^{0})$ from an input low-resolution vector $(\mathbf{I}_{\mathbf{L}})$ using the solution of least square minimization, as previously described.

Second, as a simulation stage, which verifies the face hallucination accuracy of the example-based reconstruction method, we simulate a low-resolution vector $(\mathbf{R}_{\mathbf{L}}^{t})$ by blurring and down-sampling the reconstructed high-resolution vector, then measuring the reconstruction error $(\mathbf{E}_{\mathbf{L}}^{t})$ between the input low-resolution vector and the simulated vector using the Euclidean distance function. Based on the error obtained, we update the current minimum error $(\mathbf{E}_{\mathbf{L}}^{\min})$ and its high-resolution result $(\mathbf{R}_{\mathbf{L}}^{\min})$. We assume that if the current reconstruction is successful, the reconstruction error (measured distance) is very small. Based on this assumption, we make three comparisons: whether the reconstruction is accurate, based on the comparison of the current reconstruction error to a threshold value (δ_1); whether the current iteration is inferior, based on the comparison of changes of the minimum reconstruction error and current error to a second threshold value (δ_2); whether the iteration is convergent, based on the comparison of changes of the previous distance and current distances to third threshold value (δ_3). If at least one comparison satisfies the condition, the current minimum result of face hallucination is considered as the final high-resolution vector, whereas, if no comparisons satisfy the conditions the subsequent error back-projection stage is implemented. These threshold values are determined by trial-and-error from an examination of the results of training data. If we use a small value of δ_1, or a large value of δ_2, or a small value of δ_3, there will only be a few iterations.

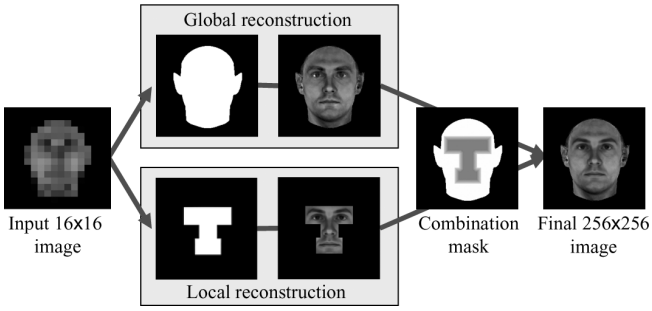

Fig. 6. Examples of global and local reconstructions for region-based face hallucination method.

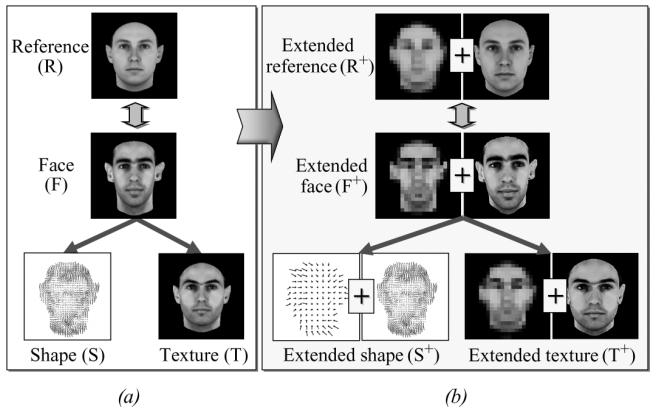

Fig. 7. Comparison of existing morphable face model and an extended morphable face model I: (a) 2-D morphable face model; (b) extended 2-D morphable face model I.

Third, as an error back-projection stage, we create a low-resolution difference vector $(\mathbf{D}_\mathbf{L}^t)$ between the input low-resolution vector and the simulated low-resolution vector, by performing a simple pixel-wise difference operation. Subsequently, the reconstruction of the high-resolution difference vector $(\mathbf{D}_\mathbf{H}^t)$ is performed by applying a similar procedure to the example-based reconstruction from the low-resolution difference vectors. In this procedure, we also constructed prototype difference vectors from example difference vectors using the leave-one-out method in the training set. Then, we compensate for the previously estimated optimal high-resolution vector by including the currently reconstructed high-resolution difference vector. In this stage, we use the weight value (w_t), according to the current error. That is, if the error is large, the weight is also large. Here, the weight value is constrained to be less than 1, to prevent divergence of iterations.

C. Region-Based Face Hallucination Method

The previously described face hallucination method is applied to the entire region of the facial image. As expected, global reconstruction methods have the drawback that various significant features affect other regions' results. Therefore, characteristics of each local image are degraded in the reconstructed high-resolution facial image.

In order to preserve characteristics of local regions, we applied the proposed example-based hallucination method to important local regions, such as the eyes, nose, and mouth. The determination of types of local masks is dependent on the purpose of the hallucination. For seamless and natural images, a large mask such as a T-shaped mask is useful. Meanwhile, for small hallucination errors, each local mask is used independently. Fig. 6 shows an example of a global mask and a local mask for the proposed region-based reconstruction method, where the local mask is a T-shaped weighted image that contains the eyes, nose, and mouth regions.

For region-based applications, it is important to obtain seamless and natural images. Blending is performed to merge different regions, which were separately reconstructed for different regions of the face, such as the eyes, nose, and mouth.

In the proposed method, the transition area is defined by the distance (D) from the boundary of the local region, for every pixel in the local region. Equivalently, the weight for merging the local reconstruction with the global reconstruction is determined as the minimum distance to the boundary of the local region.

The blending weights of the local region are computed by the following equation:

$$\begin{aligned} &\omega(x_j) = 1/(D - d(x_j) + 1), \quad \text{for } 0 < d(x_j) < D \\ &\omega(x_j) = 1, \quad \text{for } d(x_j) \geq D \end{aligned} \tag{21}$$

where $d(x_j)$ is the minimum distance from the boundary of the local feature region, and D is the minimum distance, such that $\omega(x_j) = 1$.

Then, the final value $\mathbf{R}^\mathbf{F}(x_j)$ of each pixel in the local region is computed by the following equation:

$$\mathbf{R}^\mathbf{F}(x_j) = \omega(x_j) \cdot \mathbf{R}^\mathbf{L}(x_j) + (1 - \omega(x_j)) \cdot \mathbf{R}^\mathbf{G}(x_j) \tag{20}$$

where $\mathbf{R}^\mathbf{L}(x_j)$ is the reconstructed pixel in the local region, and $\mathbf{R}^\mathbf{G}(x_j)$ is the reconstructed pixel in the global region.

D. Extended Morphable Face Model

In order to reconstruct a high-resolution facial image from a low-resolution image, we consider that an extended face is composed of an image pair comprising a low-resolution image and its corresponding high-resolution facial image, similar to the previous example-based face hallucination methods [9]–[11]. By applying the concept of an extended face to the definition of the existing morphable face model [18], an extended face is separated into an extended shape and an extended texture, as shown in Fig. 7(b).

An extended shape is represented as the vector form of (23), obtained by simply concatenating low-resolution and high-resolution shapes; L and H are the number of pixels in the low- and high-resolution faces, respectively. Similarly, an extended texture is represented as the following vector form:

$$\begin{aligned} \mathbf{S}^+ &= \left(d_1^x, d_1^y, \ldots, d_L^x, d_L^y, d_{L+1}^x, d_{L+1}^y, \ldots, d_{L+H}^x, d_{L+H}^y\right)^\mathrm{T} \\ \mathbf{T}^+ &= \left(i_1, \ldots, i_L, i_{L+1}, \ldots, i_{L+H}\right)^\mathrm{T}. \end{aligned} \tag{23}$$

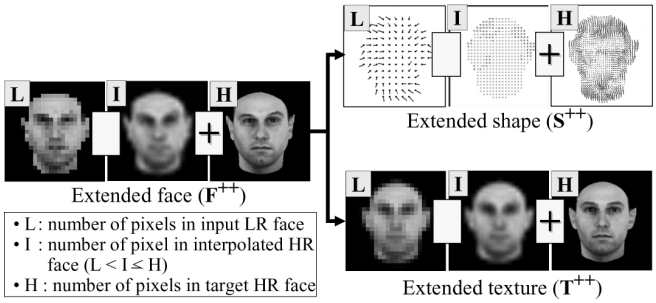

Fig. 8. Example of face representation based on the extended morphable face model II.

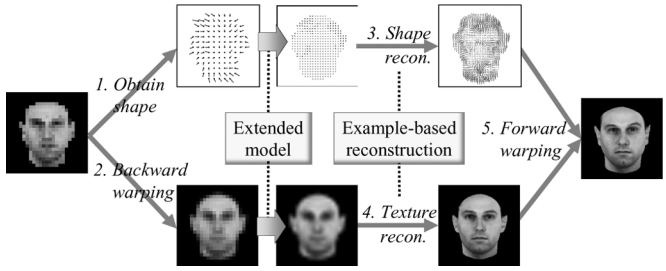

Fig. 9. Proposed example-based face hallucination method using the extended morphable face model II.

Then, by applying the example-based representation to both the extended shape $\mathbf{S}^{+}$ and extended texture $\mathbf{T}^{+}$, the following extended shape and extended texture is obtained:

$$\mathbf{S}^{+} \cong \vec{\beta} \cdot \mathbf{S}^{\mathbf{P}+}, \quad \mathbf{T}^{+} \cong \vec{\gamma} \cdot \mathbf{T}^{\mathbf{P}+} \tag{24}$$

where $\mathbf{S}^{\mathbf{P}+}$ and $\mathbf{T}^{\mathbf{P}+}$ are the extended prototype shape and texture vectors obtained from pair-wise examples of low- and high-resolution shapes, and low- and high-resolution textures, respectively.

An extended facial image is composed of an image pair comprising a low-resolution facial image and its corresponding high-resolution facial image, according to the previously defined extended morphable face model I. However, the size of a given low-resolution image varies according to capture conditions. In order to generalize the size of an input low-resolution image, we use an interpolated facial image, instead of the given low-resolution facial image. Furthermore, we apply the same interpolation methods to the extended shape and texture vectors. We term this extended model as extended morphable face model II. According to the above extension, we can define the extended shape $\mathbf{S}^{++}$ and extended texture $\mathbf{T}^{++}$ as follows:

$$\begin{aligned} \mathbf{S}^{++} &= \left(d_1^x, d_1^y, \ldots, d_I^x, d_I^y, d_{I+1}^x, d_{I+1}^y, \ldots, d_{I+H}^x, d_{I+H}^y\right)^{\mathrm{T}} \\ \mathbf{T}^{++} &= \left(i_1, \ldots, i_I, i_{I+1}, \ldots, i_{I+H}\right)^{\mathrm{T}} \end{aligned} \tag{25}$$

where I and H are the number of pixels in the interpolated image and high-resolution image, respectively.

Fig. 8 shows an example of the facial image defined by the proposed extended morphable face model II, where the bicubic interpolation method is used for the low-resolution shape and texture vectors, respectively.

The proposed example-based face hallucination method is summarized in the following procedure, by applying the definition of extended morphable face model II, as shown in Fig. 9.

- Step 1: Obtain the shape (displacement) among the pixels in an input low-resolution face corresponding to the pixels in the reference face
- Step 2: Obtain the texture of a low-resolution facial image by backward warping
- Step 3: Estimate a high-resolution shape from the interpolated high-resolution shape using the proposed example-based reconstruction method
- Step 4: Estimate a high-resolution texture from the interpolated high-resolution texture using the proposed example-based reconstruction method
- Step 5: Synthesize a high-resolution facial image by forward warping the estimated texture with the estimated shape

In the above procedure, obtaining an accurate low-resolution shape is a very difficult procedure. We can obtain low-resolution shapes by applying a 7×7 Gaussian filter with $\sigma = 0.85$, and down-sampling high-resolution shapes from in the Max-Planck Institute (MPI) database, whereas the low-resolution shapes of other databases were semi-algorithmically obtained from interpolated 64×64 facial images, as numerous researchers used several manually obtained features in high-resolution facial images [11]–[14].

IV. Experimental Results and Analysis

A. Experimental Data

To test the performance of our face hallucination method, we used the Max-Planck Institute face database (MPI DB), in which 200 facial images of Caucasian faces were rendered from a database of 3-D head models recorded by a laser scanner [18]. The original images were color images with a size of 256×256 pixels. The correspondences between a reference facial image and every facial image in the database are defined [18].

In order to verify the potential of the proposed face hallucination method, we performed tests with two other face databases, the Korean face database (KF DB) [25] and the XM2VTS database [26]. We used 540 frontal facial images of the KF DB and 295 facial images within session 1 of the XM2VTS DB. We aim to use only one image per person, in order to show that the proposed method can be generalized. Then, facial regions were manually extracted by determining the centers of both eyes, converting them to grayscale, and resizing them to 256×256 facial images. The reference face and examples from KF DB and XM2VTS DB are shown in Fig. 10.

High-resolution images were blurred using a 7×7 Gaussian filter with $\sigma = 0.85$, and down-sampled to low resolution 16×16 images by bicubic interpolation. Then, PCA was applied to a random subset of half of the facial images to construct the prototypes of each DB. This was followed by the selection of a number of Eigen-vectors (prototypes) to preserve 90% of the variances. The remaining images were used for testing our face hallucination method for each database. We also selected 100 images from each database to construct a training set for the combined database (Combined DB).

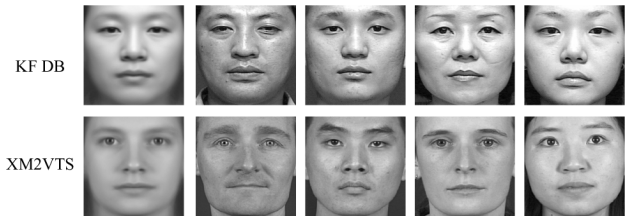

Fig. 10. Reference face and example faces from KF and XM2VTS DBs.

TABLE I
COMPARISON OF THE NUMBER OF PIXELS AND ABSOLUTE PROCESSING TIME REQUIRED BY VARIOUS HALLUCINATION METHODS

	Number of pixels	Processing time (sec.)
Bicubic	L x L	0.169
PCA	L x L	0.030
PRG	L x L + number(L-local region)	0.041
PEE	3(I x I)	0.928
PRE	3(I x I + number(I-local region))	0.971

B. Resolution Enhancement Experiments

As mentioned above, the 2-D shape and texture of the facial images were treated independently. Therefore, each high-resolution facial image was reconstructed by forward warping the reconstructed high-resolution texture with the reconstructed high-resolution shape.

In order to verify the performance of the proposed method, we compared the performance of various face hallucination methods as follows.

- Input: Nearest neighbor interpolation method
- Bicubic: Bicubic interpolation method
- PCA: Traditional example-based method using PCA transformation [3] with the general face model
- PRG: Proposed region-based method with the general face model
- PEE: Proposed example-based method with the extended morphable face model
- PRE: Proposed region-based method with the extended morphable face model

As expected, the number of pixels used for face hallucination varied according to the face model, as summarized in Table I. We also compared the absolute processing time required by each hallucination method, where the training time was not considered. We implemented each method using MATLAB software and tested it on an Intel Pentium IV system with a clock speed of 3 GHz and 2-GB main memory. As shown in the table, the proposed method reconstructs a high-resolution image within 1 s.

Fig. 11 shows examples of 256×256 high-resolution facial images reconstructed from 16×16 low-resolution images that are not included in the training set. Fig. 11(a) shows the input low-resolution images from different databases. Fig. 11(g) shows the original high-resolution facial images, and Fig. 11(b)–(f) shows the reconstructed high-resolution images using the bicubic interpolation, existing example-based hallucination method with the general face model [3], the proposed region-based face hallucination method with the general face model, the proposed example-based face hallucination method with the extended morphable face model, and the proposed region-based face hallucination method with the extended morphable face model, respectively.

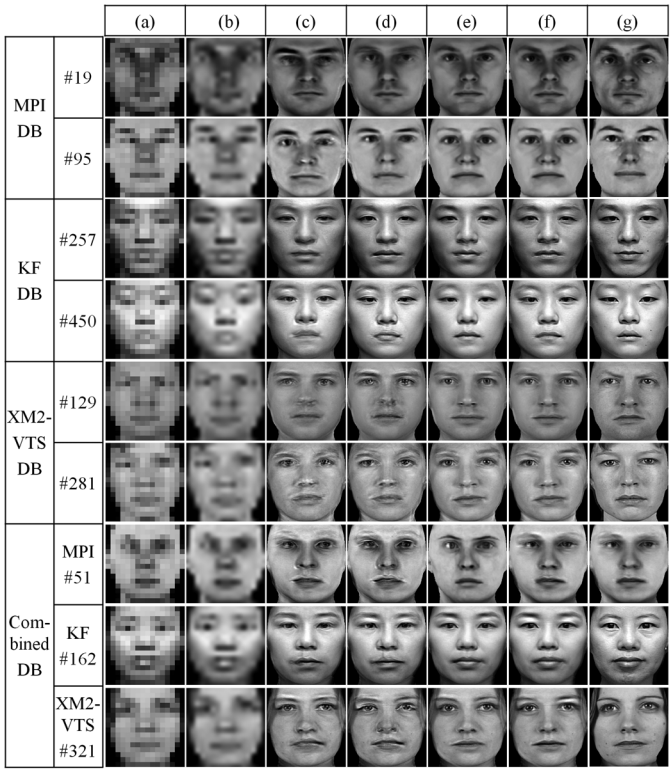

Fig. 11. Examples of 256×256 high-resolution facial images reconstructed from 16×16 low-resolution facial images in MPI, KF, XM2VTS, and combined DBs. (a) Input, (b) bicubic, (c) PCA, (d) PRG, (e) PEE, (f) PRE, and (g) original.

As shown in Fig. 11, the classification of each input low-resolution face from low-resolution images is almost impossible, even using bicubic interpolation. On the other hand, the similarity between facial images reconstructed by example-based learning methods (especially images reconstructed by the proposed region-based face hallucination method with the extended morphable face model) and the original faces is greater than that between the images reconstructed by other methods and the original faces. As shown, we also obtained similar results from the combined database.

For quantitative evaluation of various face hallucination methods, we measured the mean intensity error per pixel between the original high-resolution facial images and their reconstructed versions: the input image with nearest neighbor interpolation, bicubic interpolation method, example-based face hallucination method using the general face model (PCA), the proposed region-based hallucination method with the general face model (PRG), the proposed example-based with the extended morphable face model (PEE), and the proposed region-based method with the extended morphable face model (PRE). As shown in Fig. 12, we reduce mean reconstruction errors by using the proposed extended morphable face models, particularly the region-based hallucination method with the extended morphable face model (PRE).

We compared another quantitative evaluation measure, the structural similarity (SSIM) index [27], [28], in terms of visual image quality assessment, where the following three

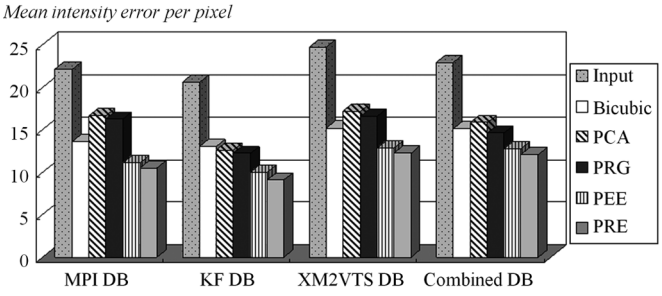

Fig. 12. Comparison of mean reconstruction errors of various hallucination methods.

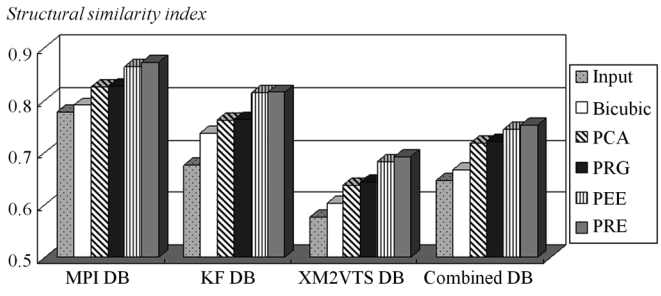

Fig. 13. Comparison of the structural similarity (SSIM) index for image quality assessments of different methods.

TABLE II
COMPARISON OF AVERAGE UNIQUENESS OF DIFFERENT HALLUCINATION METHODS

	MPI DB	KF DB	XM2VTS DB	Combined DB
Input	12.779	21.082	10.699	33.012
Bicubic	13.874	21.050	10.303	33.274
PCA	12.517	24.165	11.616	39.677
PRG	12.823	24.318	11.552	40.785
PEE	19.680	27.989	12.839	43.782
PRE	19.760	29.724	13.031	43.938
Original	20.954	31.182	15.763	49.966

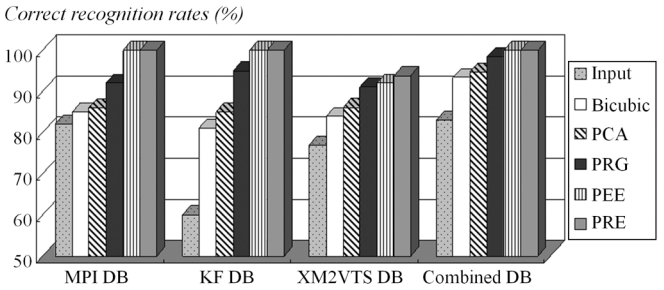

Fig. 14. Comparisons of recognition performance using the eigenface method.

parameters were considered: $K = [0.030.03]$, window $=$ fspecial(`gaussian', $9, 0.8$) and $L = 255$. This measure is based on the degradation of structural information. If two images are the same it equals 1. As shown in Fig. 13, the proposed region-based method with the extended morphable face model (PRE) outperforms the traditional example-based method with the general face model in the terms of the structural similarity index.

In order to verify the uniqueness of enhanced facial images, we measured the average distance between each facial image and other facial images in the same reconstruction results, as shown in Fig. 11(a)–(g). The uniqueness of each image is defined by the following equation:

$$U_i = \text{mean}(|R_i - R_j|), \quad j = 1, 2, \ldots, J, \quad j \neq i \qquad (26)$$

where R_i and R_j are the ith and jth facial images in each image set, respectively, and $|R_i - R_j|$ is the mean intensity difference per pixel between two images.

Table II compares the average uniqueness of different hallucination methods with MPI, KF, XM2VTS, and Combined DBs. As shown in the table, the images obtained by the proposed region-based reconstruction method using an extended morphable face model achieved better results than others.

C. Face Recognition Experiments

The comparison results of the different hallucination methods demonstrate the potential for improving the performance of face recognition systems, by reconstructing high-resolution facial images from single-frame, low-resolution facial images.

In order to verify the effect of face hallucination, we performed a face recognition experiment using the eigenface method. In the experiment, we trained the PCA space from the same training images as in the reconstruction experiments, then, extracted PCA coefficients as feature vector of a facial image [29] and measured the Euclidean distance for classification. The original 256×256 facial images were enrolled into the recognition system, and reconstructed high-resolution facial images from the 16×16 facial images were used as test data. Fig. 14 shows the correct recognition rates of the face recognition experiments with MPI, KF, XM2VTS, and combined DBs. As the figure shows, the recognition performance was improved by utilizing the proposed example-based face hallucination method.

D. Effect of Misalignment

In this paper, we described and tested the proposed example-based face hallucination method based on two assumptions. One is that low-resolution facial images were previously extracted by manual or algorithmic operations. The other is that low-resolution shapes were also obtained from given data or semi-algorithmically defined data. In order to simulate a real-world environment we considered both face detection errors and shape estimation errors for test data, and measured reconstruction errors and SSIM indices in the same manner.

First, we synthesized new test facial low-resolution images, which were considered as the results of face detection errors, by translating high-resolution facial images on the x and y axes, respectively. Translation size (offset) varied from -1 to $+1$ pixel for 16×16 resolution images. That is, face detection errors occurred between -1 to $+1$ pixel for 16×16 low-resolution facial images. In this experiment we used the KF database and the

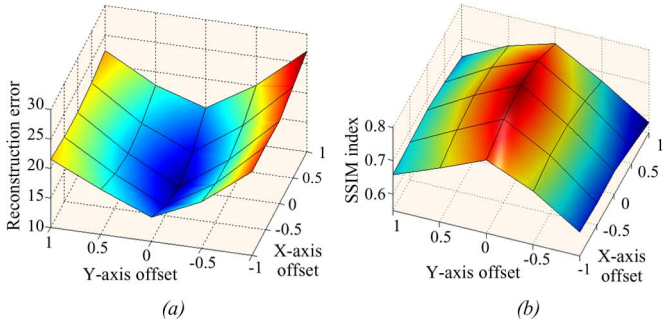

Fig. 15. Changes of the reconstruction errors and the SSIM indices with the offset of a misaligned face from original facial regions at (0, 0). (a) Changes of reconstruction errors. (b) Changes of structural similarity (SSIM) indices.

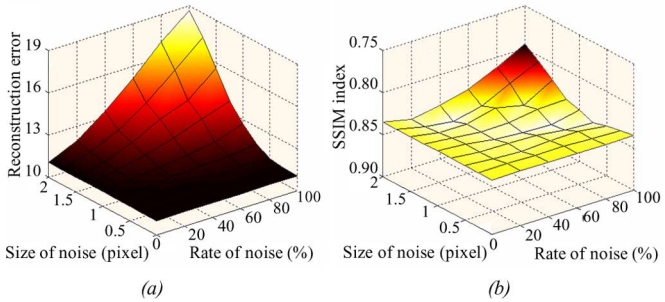

Fig. 16. Changes of the reconstruction errors and the SSIM indices with respect to shape errors. (a) Changes of reconstruction errors. (b) Changes of structural similarity (SSIM) indices.

proposed example-based face hallucination method with the extended morphable face model. As shown in Fig. 15, reconstruction errors were greater than for the original face at (0, 0), as the size of the offset is large. Also, the SSIM index was inferior, as the size of the offset is large. The results are more sensitive to variations of the y axis than the x axis, as seems likely based on characteristics of facial images.

We also synthesized new test low-resolution facial images, which were considered as the results of shape estimation errors, by including random noise in x and y shape vectors, respectively. Then changes of reconstruction errors and the SSIM indices were measured, as shown in Fig. 16, while noise frequency varied upto 100% and the magnitude of noise was randomly selected to be between -2 and $+2$ on the x and y axes for 16×16 resolution images, respectively. For example, if the noise frequency varied by 50% and the magnitude of noise is 1, we created 128 noise elements, for which values are randomly selected to be between -1 and $+1$, and the mean of absolute noise values is close to 0.5. In this experiment we used the MPI face database and the proposed example-based face hallucination method with the extended morphable face model. Reconstruction errors were affected by shape errors, but SSIM indices are less sensitive to shape variations.

V. Concluding Remarks and Further Research

In this paper, we presented an elaborate face hallucination method for reconstructing a high-resolution facial image from a single-frame, low-resolution facial image using an example-based reconstruction method with an extended morphable face model. The proposed example-based face hallucination method initially consists of the following two steps: 1) estimation of linear coefficients that minimize the error between the input low-resolution facial image and the approximated image by a linear combination of prototypes in low-resolution images, and 2) application of these estimated coefficients to high-resolution prototypes. Moreover, we applied the recursive error back-projection method to compensate for residual errors, and the region-based reconstruction method to preserve local characteristics of facial images. In addition, we utilized the morphable face model to face hallucination by defining an extended morphable face model. In this model, an extended face is composed of the interpolated high-resolution face from the input low-resolution face, and its high-resolution equivalent, then, the face is separated into an extended shape and an extended texture.

The results of the reconstruction from MPI DB consist of very natural and realistic facial images, which preserve the characteristics of individual facial components in the original high-resolution facial images. Similar results were obtained from KF, XM2VTS, and combined DBs. These results suggest that the example-based face hallucination method improves the performance of face recognition systems, especially for enhancement of the resolution of single-frame, low-resolution facial images.

The current results were obtained with synthesized, low-resolution facial images by blurring with a Gaussian filter and down-sampling high-resolution images from well-configured-facial databases. However, in order to apply the proposed example-based face hallucination methods to the real-world environment of visual surveillance systems, we must rigorously examine these methods with databases containing images captured by real-world surveillance systems. There must be further studies on shape estimation with fractional accuracy from low-resolution facial images for the resolution enhancement of captured images in real-world, low-resolution situations.

Acknowledgment

The authors would like to thank the anonymous referees for helpful comments and the Max-Planck Institute for providing the MPI face database.

References

[1] S. Baker and T. Kanade, "Limits on super-resolution and how to break them," *IEEE Trans. Pattern Anal. Mach. Intell.*, vol. 24, no. 9, pp. 1167–1183, Sep. 2002.

[2] S. C. Park, M. K. Park, and M. G. Kang, "Super-resolution image reconstruction: A technical overview," *IEEE Signal Process. Mag.*, vol. 20, no. 3, pp. 21–36, Mar. 2003.

[3] X. Wang and X. Tang, "Hallucinating face by eigentransform," *IEEE Trans. Syst., Man, Cybern. C, Appl. Rev.*, vol. 35, no. 3, pp. 425–434, Mar. 2005.

[4] G. Dedeoglu, T. Kanade, and J. August, "High-zoom video hallucination by exploiting spatio-temporal regularities," in *Proc. IEEE Conf. Computer Vision and Pattern Recognition*, Washington, DC, Jun. 2004, vol. 2, pp. 151–158.

[5] F. Dekeyser, P. Perez, and P. Bouthemy, "Restoration of noisy, blurred, undersampled image sequences using parametric motion model," in *Proc. Int. Symp. Image/Video Communications Over Fixed and Mobile Networks*, Rabat, Morocco, Apr. 2000, pp. 1071–1073.

[6] M. Elad and A. Feuer, "Restoration of a single superresolution image from several blurred, noisy, and undersampled measured images," *IEEE Trans. Image Process.*, vol. 6, no. 12, pp. 1646–1658, Dec. 1997.

[7] R. C. Hardie, K. J. Barnar, and E. E. Armstrong, "Joint map registration and high-resolution image estimation using a sequence of undersampled images," *IEEE Trans. Image Process.*, vol. 6, no. 12, pp. 1621–1633, Dec. 1997.
[8] T. A. Stephenson and T. Chen, "Adaptive Markov random fields for example-based super-resolution of faces," *EURASIP J. Appl. Signal Process.*, vol. 2006, pp. 1–11, 2006, Article ID 31062.
[9] B. K. Gunturk, A. U. Batur, Y. Altunbasak, M. H. Hayes, and R. M. Mersereau, "Eigenface-domain super-resolution for face recognition," *IEEE Trans. Image Process.*, vol. 12, no. 5, pp. 597–606, May 2003.
[10] C. Liu, H.-Y. Shum, and C.-S. Zhang, "A two-step approach to hallucinating faces: Global parametric model and local nonparametric model," in *Proc. IEEE Conf. Computer Vision and Pattern Recognition*, Dec. 2001, vol. 1, pp. 192–198.
[11] Y. Li and X. Lin, "An improved two-step approach to hallucinating faces," in *Proc. IEEE Conf. Image and Graphics*, Dec. 2004, pp. 298–301.
[12] Y. Li and X. Lin, "Face hallucination with pose variation," in *Proc. 6th IEEE Conf. Automatic Face and Gesture Recognition*, Seoul, Korea, May 2004, pp. 723–728.
[13] W. Liu, D. Lin, and X. Tang, "Hallucinating faces: TensorPatch super-resolution and coupled residue compensation," in *Proc. IEEE Conf. Computer Vision and Pattern Recognition*, San Diego, CA, Jun. 2005, vol. 2, pp. 478–484.
[14] W. Liu, X. Tang, and J. Liu, "Bayesian tensor inference for sketch-based facial photo hallucination," in *Proc. 20th Int. Joint Conf. Artificial Intelligence*, Hyderabad, India, Jan. 2007, pp. 2141–2146.
[15] J.-S. Park and S.-W. Lee, "Resolution enhancement of facial image using an error back-projection of example-based learning," in *Proc. 6th IEEE Conf. Automatic Face and Gesture Recognition*, Seoul, Korea, May 2004, pp. 831–836.
[16] H. Sato, W. Freeman, and A. Onozawa, "Quality improvement for intermediate views using example-based super-resolution," *NTT Tech. Rev.*, vol. 1, no. 6, pp. 44–47, Sep. 2003.
[17] C. Liu, H.-Y. Shum, and W. T. Freeman, "Face hallucination: Theory and practice," *Int. J. Comput. Vis.*, vol. 75, no. 1, pp. 115–134, 2007.
[18] T. Vetter and N. E. Troje, "Separation of texture and shape in images of faces for image coding and synthesis," *J. Opt. Soc. Amer. A*, vol. 14, no. 9, pp. 2152–2161, 1997.
[19] B.-W. Hwang and S.-W. Lee, "Reconstruction of partially damaged face images based on a morphable face model," *IEEE Trans. Pattern Anal. Mach. Intell.*, vol. 25, no. 3, pp. 365–372, Mar. 2003.
[20] V. Blanz and T. Vetter, "Face recognition based on fitting a 3D morphable model," *IEEE Trans. Pattern Anal. Mach. Intell.*, vol. 25, no. 9, pp. 1063–1074, Sep. 2003.
[21] B. Tom and A. Katsaggelos, "Resolution enhancement of monochrome and color video using motion compensation," *IEEE Trans. Image Process.*, vol. 10, no. 2, pp. 278–287, Feb. 2001.
[22] W. Liu, D. Lin, and X. Tang, "Neighbor combination and transformation for hallucinating faces," in *Proc. IEEE Conf. Multimedia and Expo*, Amsterdam, The Netherlands, Jul. 2005, pp. 145–148.
[23] M.-H. Yang, D. J. Kriegman, and N. Ahuja, "Detecting faces in images: A survey," *IEEE Trans. Pattern Anal. Mach. Intell.*, vol. 24, no. 1, pp. 34–58, Jan. 2002.
[24] P. Kakumanua, S. Makrogiannisa, and N. Bourbakis, "A survey of skin-color modeling and detection methods," *Pattern Recognit.*, vol. 40, no. 3, pp. 1106–1122, Mar. 2007.
[25] M.-C. Roh and S.-W. Lee, "Performance analysis of face recognition algorithms on Korean face database," *Int. J. Pattern Recognit. Artif. Intell.*, vol. 21, no. 6, pp. 1017–1033, 2007.
[26] [Online]. Available: http://www.ee.surrey.ac.uk/CVSSP/xm2vtsdb/
[27] Z. Wang, A. C. Bovik, H. R. Sheikh, and E. P. Simoncelli, "Image quality assessment: From error visibility to structural similarity," *IEEE Trans. Image Process.*, vol. 13, no. 4, pp. 600–612, Apr. 2004.
[28] [Online]. Available: http://www.cns.nyu.edu/~lcv/ssim/
[29] M. A. Turk and A. P. Pentland, "Eigenfaces for recognition," *J. Cogn. Neurosci.*, vol. 3, no. 1, pp. 71–86, 1991.

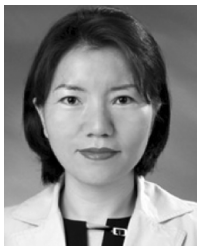

Jeong-Seon Park (M'07) received the B.S. and M.S. degrees in computer science from Chungbuk National University, Cheongju, Korea, in 1988 and 1992, respectively, and the Ph.D. degree in computer science from Korea University, Seoul, Korea, in 2005.

From 1994 to 1999, she was a Research Engineer at Hyundai Information Technology Co., Ltd., Gyeonggi, Korea. In 2005, she joined the faculty of the Department of Multimedia, Chonnam National University, Yeosu, Korea, as a full-time Lecturer, and she is now an Assistant Professor. Her research interests include pattern recognition, image processing, and computer vision.

Dr. Park won third and second place, respectively, in the Annual Best Student Paper Award of the Korea Information Science Society in 1994 and 2004, respectively. She received the fourth place award from the Samsung Human Tech Paper Contest from Samsung Electronics in 2005.

Seong-Whan Lee (S'84–M'89–SM'96) received the B.S. degree in computer science and statistics from Seoul National University, Seoul, Korea, in 1984, and the M.S. and Ph.D. degrees in computer science from KAIST in 1986 and 1989, respectively.

From 1989 to 1995, he was an Assistant Professor in the Department of Computer Science, Chungbuk National University, Cheongju, Korea. In 1995, he joined the faculty of the Department of Computer Science and Engineering, Korea University, Seoul, as an Associate Professor, and he is now a Full Professor.

Dr. Lee was the winner of the Annual Best Student Paper Award of the Korea Information Science Society in 1986. He obtained the First Outstanding Young Researcher Award at the Second International Conference on Document Analysis and Recognition in 1993, and the First Distinguished Research Award from Chungbuk National University in 1994. He also obtained the Outstanding Research Award from the Korea Information Science Society in 1996. He was the founding Co-Editor-in-Chief of the *International Journal of Document Analysis and Recognition* and has been an Associate Editor of the *Pattern Recognition Journal*, the *International Journal of Pattern Recognition and Artificial Intelligence*, and the *International Journal of Image and Graphics* since 1997. He has served on the program committees of several well-known international conferences. He is a fellow of IAPR and a life member of the Korea Information Science Society. His research interests include pattern recognition, computer vision, and neural networks. He has authored more than 250 publications in international journals and conference proceedings, as well as ten books.